Supplementary information

0D/3D nanoreactor by quantum dots and ZIF-67 for efficient urea electrosynthesis with substrate enrichment and coupling

Xuanbo Liu,[†a] Tianyao Jiang,[†a] Dongxu Zhang,[a] Xingjian Yan,[a] Tongqing Zhang,[a] Jinying Zhang,[b] Yanhong Liu,[*a] Baodong Mao,[*a]

[a] *School of Chemistry and Chemical Engineering, Jiangsu University, Zhenjiang 212013, PR China.*

[b] *State Key Laboratory of Electrical Insulation and Power Equipment, Center of Nanomaterials for Renewable Energy (CNRE), School of Electrical Engineering, Xi'an Jiaotong University, Xi'an 710049, PR China*

[*] *Corresponding authors. E-mail: liuyh@ujs.edu.cn (Y. Liu); maobd@ujs.edu.cn (B. Mao).*

[†] *These authors contributed equally to this work*

Experimental section

Materials. All chemicals were of analytical grade or higher and used as received. The following reagents were purchased from Aladdin: 2-methylimidazole, cobalt nitrate hexahydrate ($Co(NO_3)_2 \cdot 6H_2O$), cupric acetylacetonate ($Cu(acac)_2$, 97%), molybdenyl acetylacetonate ($MoO_2(acac)_2$), potassium bicarbonate ($KHCO_3$, AR), potassium nitrate (KNO_3, AR), potassium nitrite (KNO_2, AR), ammonium chloride (NH_4Cl, 99.5%), phosphoric acid (H_3PO_4, AR), iron(III) chloride ($FeCl_3$, AR), diacetyl monoxime ($C_4H_7NO_2$, AR), thiosemicarbazide (CH_5N_3S, 99%), N-(1-

naphthyl)ethylenediamine dihydrochloride ($C_{12}H_{14}N_2 \cdot 2HCl$, 98%), sodium citrate dihydrate ($C_6H_5Na_3O_7 \cdot 2H_2O$, AR), sodium hypochlorite solution (NaClO, AR), and urea (H_2NCONH_2, 99.99%). Dodecanethiol ($C_{12}H_{26}S$, 98%), sulfanilamide ($C_6H_8N_2O_2S$, 99.5%), and n-hexane were obtained from Macklin. Sulfuric acid (H_2SO_4, 95.0–98.0%) and ethanol (C_2H_6O, AR) were supplied by Sinopharm Chemical Reagent Co., Ltd.

Synthesis of ZIF-67. Following a previous literature procedure with minor modifications.[1] A solution of 8.00 mmol 2-methylimidazole in 10 mL methanol (Solution A) was prepared under magnetic stirring. Separately, 1.00 mmol of $Co(NO_3)_2 \cdot 6H_2O$ was dissolved in 10 mL methanol to form Solution B. Solution B was then rapidly poured into Solution A, and the mixture was ultrasonicated for 3 h, yielding a purple precipitate. The solid was collected, washed repeatedly with anhydrous ethanol to remove unreacted precursors, and dried in a vacuum oven at 60 °C for 10 h to obtain ZIF-67 as a purple crystalline powder.

Synthesis of $Cu_{2-x}S/MoS_2$. Under a nitrogen atmosphere, a mixture of 0.80 g $Cu(acac)_2$, 16 mg $Mo(acac)_2$, and 100 mL 1-dodecanethiol was heated at 243 °C for 30 min. After cooling to room temperature, the product was washed three times with ethanol and n-hexane, yielding $Cu_{2-x}S/MoS_2$, which was stored in an ethanol solution.

Synthesis of ZIF-67-$Cu_{2-x}S/MoS_2$-x%. A 5 $mg \cdot mL^{-1}$ dispersion of ZIF-67 was prepared by ultrasonically dispersing 100 mg of the as-synthesized ZIF-67 in 20 mL of ethanol. Ethanol solutions of $Cu_{2-x}S/MoS_2$ were then added to the ZIF-67 dispersion

with mass ratios of 50%, 70%, and 90% relative to ZIF-67. The mixtures were subjected to ultrasonication for 2 h at room temperature to obtain a series of nanocomposites. These were denoted as ZIF-67-$Cu_{2-x}S/MoS_2$-x% (x = 50, 70, 90), corresponding to ZIF-67-$Cu_{2-x}S/MoS_2$-50%, ZIF-67-$Cu_{2-x}S/MoS_2$-70%, ZIF-67-$Cu_{2-x}S/MoS_2$-90%, respectively.

Characterization Methods

Transmission electron microscopy (TEM), high-resolution TEM (HRTEM), and high-angle annular dark-field scanning transmission electron microscopy (HAADF-STEM) characterizations, along with energy-dispersive X-ray spectroscopy (EDS) analysis, were performed on a Tecnai G2 F30 S-Twin microscope (Thermo Fisher Scientific, USA). The samples were characterized by X-ray powder diffraction (XRD) by a Bruker D8 Advance diffractometer (Germany) equipped with graphite-monochromatized Cu-Kα radiation (λ=1.5418 Å). CO_2 temperature programmed desorption (CO_2-TPD) experiments were conducted on a Micromeritics AutoChem 2920 analyzer. Raman spectroscopy was performed on a Thermo Fisher DXR (Thermo Fisher, USA). Sorption isotherm for N_2: Autosorb iQ system were used to measure the specific surface area and pore structure using nitrogen as the adsorbate at 77 K. X-ray photoelectron spectroscopy (XPS) was conducted using a Thermo Scientific K-Alpha spectrometer with an Al Kα X-ray source. *In-situ* Attenuated Total Reflection Fourier Transform Infrared Spectroscopy (ATR-FTIR) testing was conducted on a Nicolet iS50 (Thermo Fisher, USA) spectrometer. First, 20 μL of the sample ink was applied onto a gold-plated silicon crystal to capture infrared signals. Subsequently, a mixed solution of 0.1

M $KHCO_3$ and 0.1 M KNO_3 was added. After purging with high-purity carbon dioxide gas for 20 minutes, an Ag/AgCl reference electrode and a platinum wire electrode were used to collect and record FTIR data at different potentials. The *in-situ* Raman spectroscopy measurements were conducted using a setup comprising a Raman microscope, a custom-designed *in-situ* electrochemical cell, and a CHI 760E electrochemical workstation. The spectroelectrochemical cell was fabricated from PTFE and featured a quartz window above the working electrode for optical access. A carbon-based substrate, serving as the working electrode, was firmly attached to a graphite plate to ensure electrical conductivity. A graphite rod and an Ag/AgCl electrode were employed as the counter and reference electrodes, respectively. During the measurements, the electrolyte—a mixture of 0.1 M $KHCO_3$ and 0.1 M KNO_3 was continuously circulated through the cell at a rate of 5 mL min^{-1}. CO_2 was purged into the electrolyte at a constant flow rate of 25 sccm. Raman spectra were collected while applying a series of cathodic potentials.

Electrochemical measurements

Electrochemical measurements were performed using a CHI 760E electrochemical workstation (Chenhua, Shanghai, China) in a standard three-electrode configuration. A custom H-type cell was employed, in which a carbon paper (0.5 × 2 cm^2) loaded with 0.1 mg of catalyst served as the working electrode, an Ag/AgCl electrode as the reference, and a Pt sheet (1 × 2 cm^2) as the counter electrode. The effect of catalyst loading on the reaction performance was systematically investigated. It was found that the highest urea production rate was obtained at 0.1 mg cm^{-2} (Fig. S6). Accordingly, this loading was chosen as the optimal condition for all subsequent electrochemical

measurements.

The two compartments were separated by a Nafion 117 membrane. The cathode chamber contained 25 mL of 0.1 M $KHCO_3$ + 0.1 M KNO_3 electrolyte, while the anode chamber was filled with 25 mL of 0.1 M $KHCO_3$. Prior to electrolysis, CO_2 (99.999%) was purged through the catholyte at a flow rate of 25 sccm for 20 min, and the gas flow was maintained throughout the experiment. Electrochemical performance was evaluated through linear sweep voltammetry (LSV), chronoamperometry (i-t), electrochemical impedance spectroscopy (EIS), and cyclic voltammetry (CV). All electrolysis tests were conducted for 1 h at a stirring rate of 150 rpm under various applied potentials. The electrochemical active surface area (ECSA) was derived from the double-layer capacitance (C_{dl}), which was determined from CV measurements. All potentials were referenced to the reversible hydrogen electrode (RHE) by

$$E_{RHE} = E_{Ag/AgCl} + 0.198\ V + 0.059 \times pH \quad (1)$$

Open-circuit potential (OCP) measurements were performed to probe the adsorption affinity of the catalysts towards NO_3^- and CO_2. After achieving a stable OCP in CO_2-saturated 0.1 M $KHCO_3$, a concentrated KNO_3 solution was injected to reach a final concentration of 0.1 M, and the OCP transient was recorded until a new steady state was reached. For CO_2 adsorption, the electrolyte was purged with CO_2 gas (25 sccm) while continuously monitoring the OCP until stabilization

Product determination

Urea concentration was quantified using the diacetyl monoxime (DAMO) colorimetric method. First, a DAMO + thiosemicarbazide (TSC) solution was prepared by

dissolving 5 g of diacetyl monoxime and 100 mg of thiosemicarbazide in distilled water, followed by dilution to 1000 mL. Separately, an acid-ferric solution was prepared by mixing 100 mL of concentrated phosphoric acid, 300 mL of concentrated sulfuric acid, and 100 mg of ferric chloride with distilled water, and diluting the mixture to 1000 mL.

For the assay, 1 mL of the electrolyte collected from the cathode compartment was combined with 2 mL of the acid-ferric solution and 1 mL of the DAMO-TSC solution. The mixture was incubated at 100 °C for 20 min. After cooling to room temperature, the absorbance of the solution at 525 nm was recorded by UV-Vis spectroscopy.

The urea yield R_{urea} and Faradaic efficiency FE_{urea} were calculated according to the following equations:

$$R_{\text{urea}}\ (\mu\text{g h}^{-1}\ \text{mg}_{\text{cat}}^{-1}) = \frac{C_{\text{urea}}\ (\mu\text{g mL}^{-1}) \times V\ (\text{mL})}{t\ (\text{h}) \times m\ (\text{mg})} \quad (2)$$

$$\text{FE}_{\text{urea}}\ (\%) = \frac{16 \times F \times C_{\text{urea}} \times V}{60.06 \times Q} \times 100\% \quad (3)$$

where C_{urea} is the measured mass concentration of urea, V is the volume of the electrolyte, t is the electrolysis time, m is the mass of the catalyst loaded on the electrode, F is the Faraday constant (96485.3 C mol^{-1}), and Q represents the total charge passed during the reaction.

For the isotopic labeling experiment, $K^{15}NO_3$ (99 atom%) was used as the electrolyte, in which the electrocatalysis test was performed at -0.6 V vs. RHE. Subsequently, the electrolyte was mixed with dimethyl sulfoxide-d_6 at a ratio of 1:9 and shaken evenly.

Finally, the measurement was performed on a Bruker NMR instrument (BRUKERAC-P400, Germany). The gas products of CO and H_2 were monitored by a gas chromatography, (FULI, GC-9790 II plus).

NH_3 concentration determination

Ammonia was quantified via the indophenol blue method. The following color-developing solutions were prepared: Solution A: 1 M NaOH containing 5 wt% sodium citrate and 5 wt% salicylic acid. Solution B: 0.05 M NaClO solution. Solution C: 0.5 g sodium nitroferricyanide dissolved in 50 mL deionized water. For analysis, 2 mL of the catholyte was mixed sequentially with 2 mL of Solution A, 1 mL of Solution B, and 0.2 mL of Solution C. The mixture was kept in the dark for 2 h, after which its absorbance at 655 nm was recorded by UV-Vis spectroscopy.

The NH_3 yield rate and Faradaic efficiency were calculated as follows:

$$R_{NH_3}\ (\mu g\ h^{-1}\ mg_{cat}^{-1}) = \frac{C_{NH_3}\ (\mu g\ mL^{-1}) \times V\ (mL)}{t\ (h) \times m\ (mg)} \quad (4)$$

$$FE_{NH_3}\ (\%) = \frac{8 \times F \times C_{NH_3} \times V}{17 \times Q} \times 100\% \quad (5)$$

where C_{NH_3} is the measured mass concentration of NH_3, V is the electrolyte volume, t is the electrolysis time, m is the catalyst mass, F is the Faraday constant (96485.3 C mol^{-1}), and Q is the total charge passed.

NO_2^- concentration determination

Nitrite concentration was determined colorimetrically using the Griess-like method.

First, a chromogenic reagent was prepared by dissolving 2 g of sulfanilamide and 0.1 g of N-(1-naphthyl)-ethylenediamine dihydrochloride in a mixture of 25 mL deionized water and 5 mL phosphoric acid, followed by dilution to 50 mL in a volumetric flask.

For the assay, 0.1 mL of the chromogenic reagent was added to a solution containing 1 mL of the electrolyte, 1 mL of deionized water, and 3 mL of saturated boric acid solution. After standing for 20 min, the absorbance at 540 nm was measured by UV-Vis spectroscopy.

The NO_2^- yield rate and Faradaic efficiency were calculated as follows:

$$R_{NO_2^-}\ (\mu g\ h^{-1}\ mg_{cat}^{-1}) = \frac{C_{NO_2^-}\ (\mu g\ mL^{-1}) \times V\ (mL)}{t\ (h) \times m\ (mg)} \quad (6)$$

$$FE_{NO_2^-}\ (\%) = \frac{2 \times F \times C_{NO_2^-} \times V}{46 \times Q} \times 100\% \quad (7)$$

where $C_{NO_2^-}$ is the measured mass concentration of NO_2^-, and other symbols retain the same definitions as above.

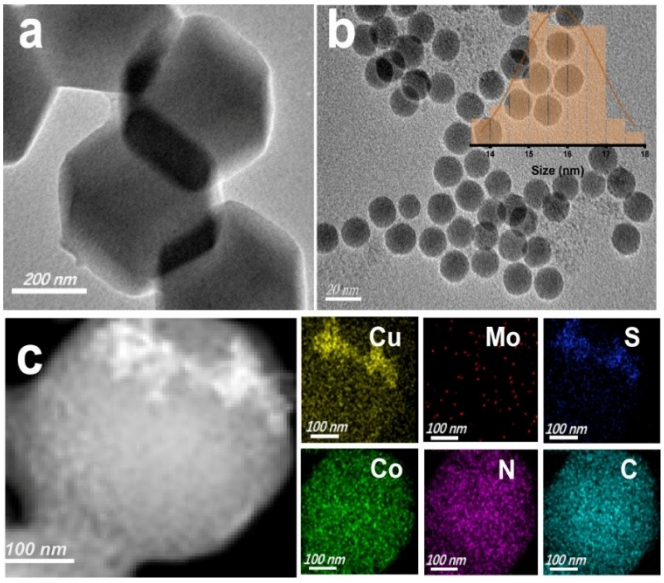

Fig. S1 TEM images of (a) ZIF-67 and (b) $Cu_{2-x}S/MoS_2$. (c) HAADF-STEM and the corresponding elemental mapping images of ZIF-67-$Cu_{2-x}S/MoS_2$. Inset in Fig. S1b: size distribution diagram of the $Cu_{2-x}S/MoS_2$ QDs.

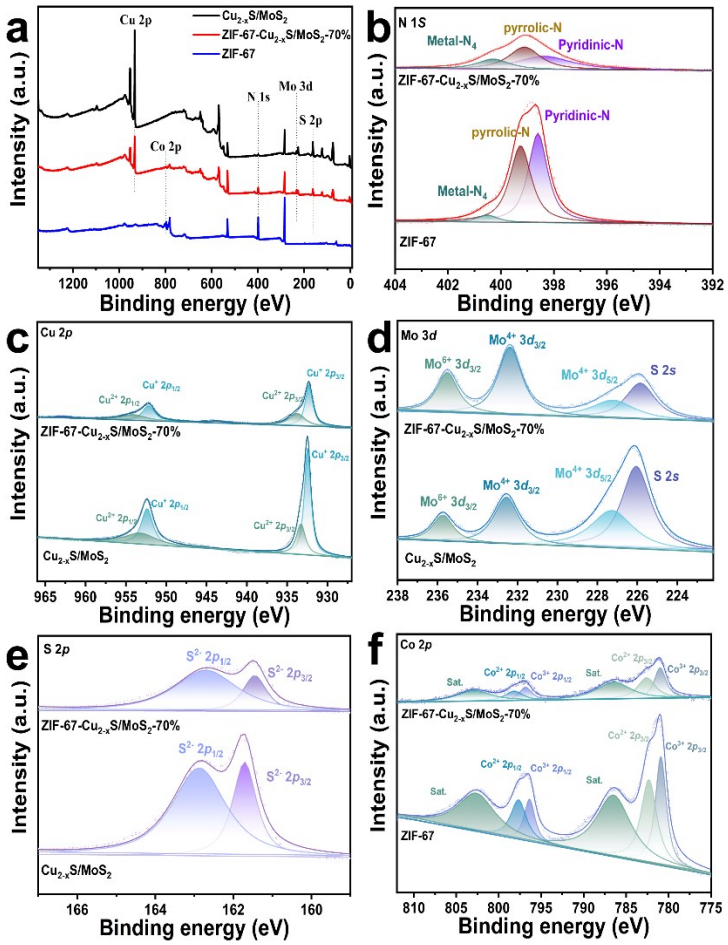

Fig. S2 (a) XPS survey spectra of ZIF-67, $Cu_{2-x}S/MoS_2$ and ZIF-67-$Cu_{2-x}S/MoS_2$-70%. High-resolution XPS spectra of (b) N 1s, (c) Cu 2p, (d) Mo 3d, (e) S 2p and (f) Co 2p.

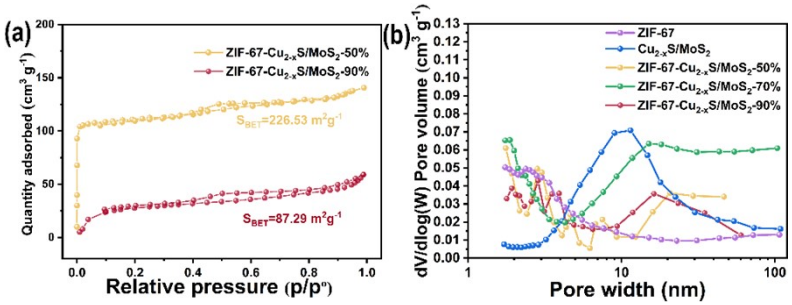

Fig. S3 (a) N_2 adsorption-desorption isotherms and (b) pore size distribution curves.

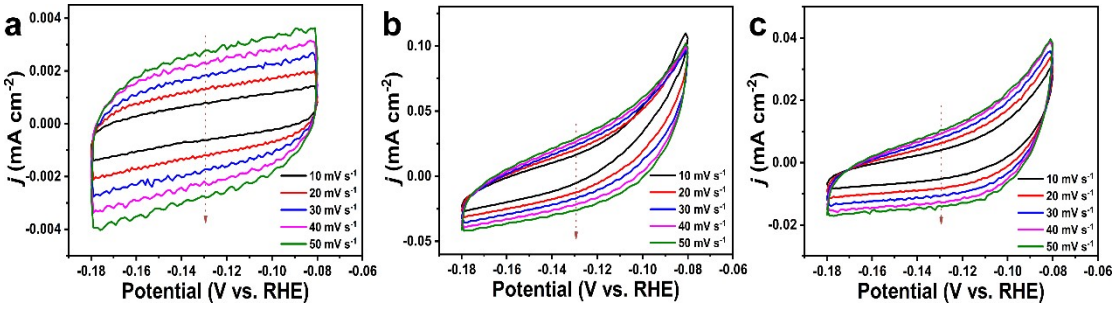

Fig. S4 CV curves of (a) ZIF-67, (b) $Cu_{2-x}S/MoS_2$, and (c) ZIF-67-$Cu_{2-x}S/MoS_2$-70%.

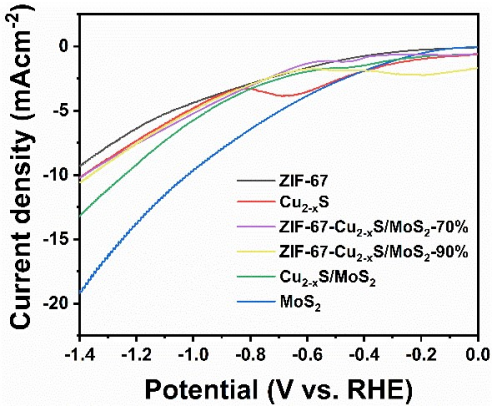

Fig. S5 LSV curves of different catalysts in the 0.1 M $KHCO_3$ electrolyte for the HER test.

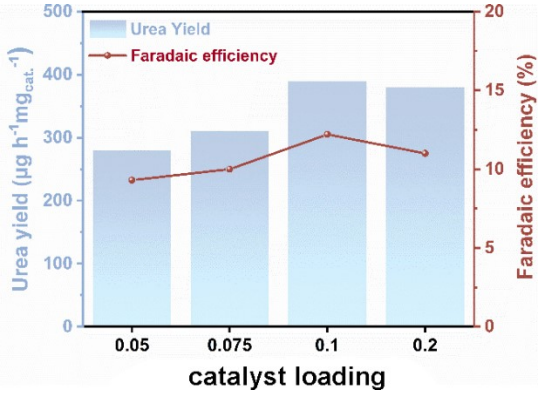

Fig. S6 Urea yields and FEs for different loadings of ZIF-67-$Cu_{2-x}S/MoS_2$-70% catalysts at -0.75 V vs. RHE.

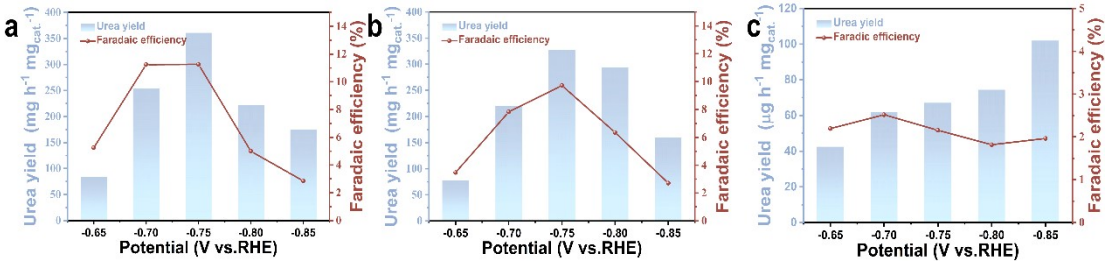

Fig. S7 (a) Urea yields and Faradaic efficiencies of (a) ZIF-67-$Cu_{2-x}S/MoS_2$-50%, (b) ZIF-67-$Cu_{2-x}S/MoS_2$-90%, and (c) $Cu_{2-x}S/MoS_2$ at various applied potentials.

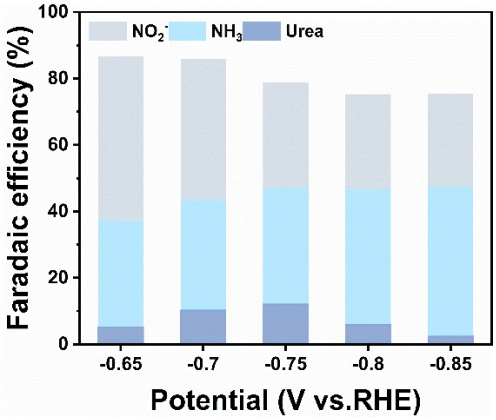

Fig. S8 Faradaic efficiencies of nitrate reduction products on the ZIF-67-$Cu_{2-x}S/MoS_2$-70% at different potentials.

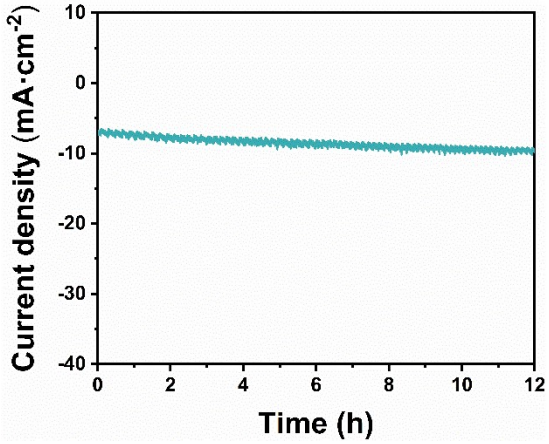

Fig. S9 The 12-h stability test at -0.75 V vs. RHE.

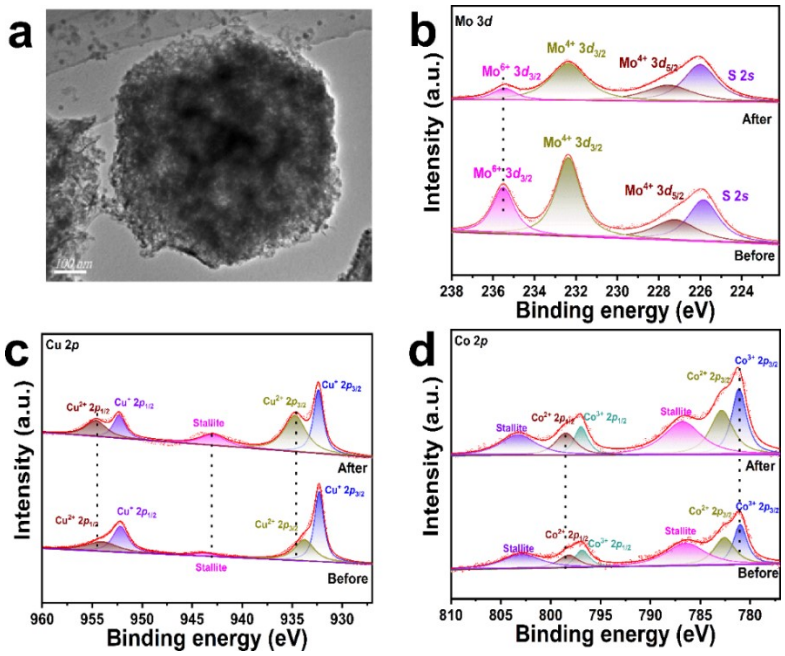

Fig. S10 (a) TEM image of ZIF-67-$Cu_{2-x}S/MoS_2$-70% after electrocatalysis. The XPS spectra of the ZIF-67-$Cu_{2-x}S/MoS_2$-70% before and after reaction: (b) Mo 3d, (c) Cu 2p, (d) Co 2p.

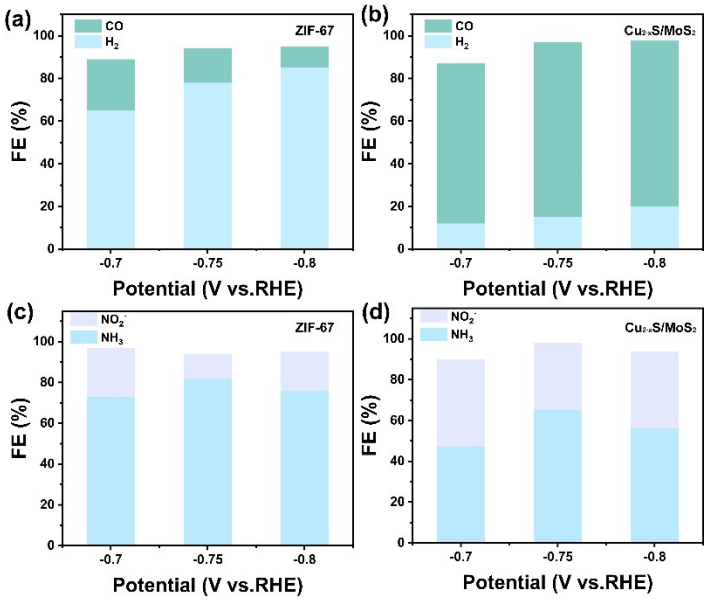

Fig. S11 FEs of the electrolytic products of ZIF-67 and $Cu_{2-x}S/MoS_2$ for (a, b) CO_2RR and (c, d) NO_3RR at different potentials.

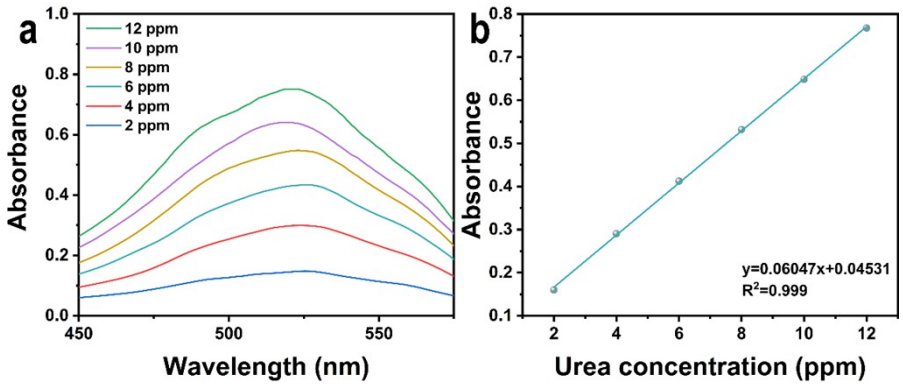

Fig. S12 (a) UV-Vis spectroscopy curves of urea solutions with different known concentration. (b) Standard curve of urea.

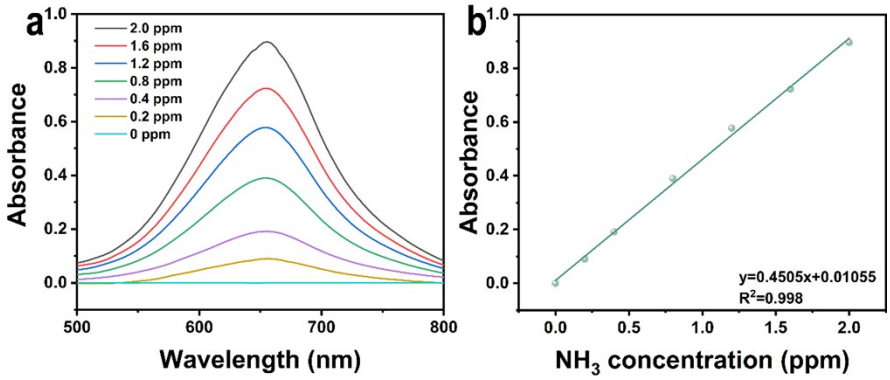

Fig. S13 (a) UV-Vis spectroscopy curves of NH_3 solutions with different known concentration. (b) Standard curve of NH_3.

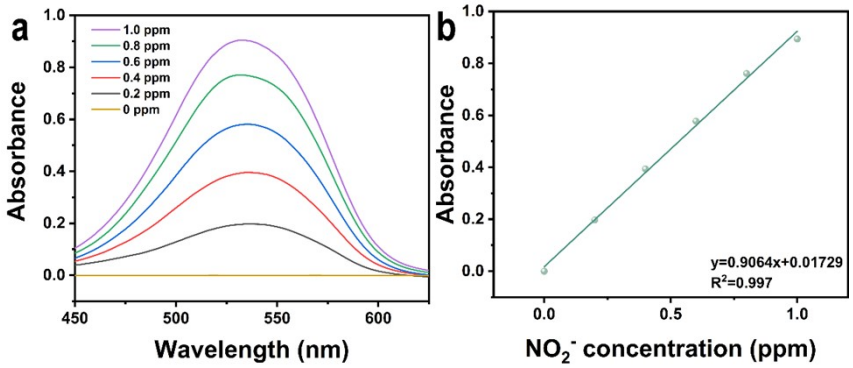

Fig. S14 (a) UV-Vis spectroscopy curves of NO_2^- solutions with different known concentration. (b) Standard curve of NO_2^-.

Table S1. Comparison of urea electrosynthesis performance of ZIF-67-$Cu_{2-x}S/MoS_2$-70% with previously reported electrocatalysts.

Catalyst	Potential (V vs. RHE)	FE_{urea}	$Yield_{urea}$ (μg h^{-1} mg_{cat}^{-1})	Eletrolyte	Ref
ZIF-67-$Cu_{2-x}S/MoS_2$-70%	-0.7	12%	600	CO_2-saturated 0.1 M $KHCO_3$+0.1 M KNO_3	This Work
AuPd	-0.5	15.6%	204.3	0.75 M $KHCO_3$+ 0.25 M KNO_3	2
biCoPc	-0.7	47.4%	24.5	CO_2-saturated 0.2 M $KHCO_3$+0.02 M KNO_2	3
a-$Cu_{0.1}CoB_x$ metallene	-0.5	27.7%	312	CO_2-saturated 0.1 M KNO_2	4
TiO_2–Nafion	-0.5 V	40%	264	CO_2-saturated 0.1 M KNO_2	5
Ru-Cu CF	0.13	25.4%	151.6	CO_2-saturated 0.1 M KNO_2	6
$CuWO_4$	-0.2	70.1 %	100	CO_2-saturated 0.1 M KNO_3	7
F-rich CNT	-0.65	18%	382.0	CO_2-saturated 0.1 M KNO_3	8
SnO_2CuCo	-0.4	50%	162.3	CO_2-saturated 0.1 M KNO_3	9
Cu-MOF-CQD	-0.5	18.5%	260.2	0.1 M $KHCO_3$+0.04 M KNO_3	10
Fe-TPP/CNTs	-0.8	6.57%	1678	0.2 M $KHCO_3$ + 0.1 M KNO_3	11

■ REFERENCES

1. P. Maurya, V. Vyas, A. N. Singh and A. Indra, *Chem Commun*, 2023, **59**, 7200-7203.
2. H. Wang, Y. Jiang, S. Li, F. Gou, X. Liu, Y. Jiang, W. Luo, W. Shen, R. He and M. Li, *Appl Catal, B*, 2022, **318**, 121819.
3. R. Zhang, W. Hu, J. Liu, K. Xu, Y. Liu, Y. Yao, M. Liu, X. G. Zhang, H. Li, P. He and S. Huo, *Small*, 2024, **20**, 2403285.
4. Y. Wu, H. Lin, Q. Mao, H. Yu, K. Deng, J. Wang, L. Wang, Z. Wang and H. Wang, *Small*, 2024, **20**, 2407679.
5. D. Saravanakumar, J. Song, S. Lee, N. H. Hur and W. Shin, *ChemSusChem*, 2017, **10**, 3999-4003.
6. J. Qin, N. Liu, L. Chen, K. Wu, Q. Zhao, B. Liu and Z. Ye, *ACS Sustainable Chem Eng*, 2022, **10**, 15869-15875.
7. Y. Zhao, Y. Ding, W. Li, C. Liu, Y. Li, Z. Zhao, Y. Shan, F. Li, L. Sun and F. Li, *Nat Commun*, 2023, **14**, 4491.
8. X. Liu, P. V. Kumar, Q. Chen, L. Zhao, F. Ye, X. Ma, D. Liu, X. Chen, L. Dai and C. Hu, *Appl Catal, B*, 2022, **316**, 121618.
9. T. Zhang, P. Wang, C. Yang, Y. Gao, J. Yao, S. Meng, H. Li, R. Tan, J. Liu and Z. Li, *J Am Chem Soc*, 2025, **147**, 33108-33119.
10. Y. Li, K. Huang, W. Liu, K. Wang, S. Fu, H. Guo, J. Zhang, C. Lian and L. Wang, *J Colloid Interface Sci*, 2026, **703**, 139264.
11. Q. Hu, W. Zhou, S. Qi, Q. Huo, X. Li, M. Lv, X. Chen, C. Feng, J. Yu, X. Chai, H. Yang and C. He, *Nature Sustainability*, 2024, **7**, 442-451.